ULB UNIVERSITÉ LIBRE DE BRUXELLES

ULB BRUFACE BRUSSELS FACULTY OF ENGINEERING VUB

VUB VRIJE UNIVERSITEIT BRUSSEL

ELEC-H415

Modeling A Vehicle-to-Vehicle Communication Channel in an Urban Environment

Author :
Cédric Sipakam

Teacher :
Philippe de Doncker

2025

Contents

List of Figures

List of Tables

Introduction

For their first year of master in Electrical Engineering and Information Technology in the Bruface program, students were asked to do a project for their communication channels course. The project consists of modelling a vehicle-to-vehicle wireless communication channel. The analysis is grounded in an urban canyon scenario where two vehicles, equipped with vertical $\lambda/2$ dipole antennas, travel along the center of a 20-meter wide street surrounded by building with a relative permittivity of $\epsilon_r = 4$. The distance d between the vehicles is variable and can be maximum $d_{max} = 1km$

The communication system operated at a carrier frequency of $f_c = 5.9GHz$ with a bandwidth of $B_{RF} = 1000MHz$ and a transmitter power of $P_{TX} = 0.1W$. This report develops the channel model from basic principles, progressing through narrowband and wideband analyses of both Line-of-Sight and full multiray conditions, with an emphasis on the mathematical derivations and physical interpretation of the results.

1

Theoretical Preliminaries

An antenna is an electrical component that acts as a transducer between a guided electrical signal and a propagating electromagnetic wave. To analyze its behavior within an electrical system, an equivalent circuit was drawn. In transmission mode, a signal source feeds the antenna, which has an impedance Z_a. This impedance consists of the sum between a radiation resistance R_{ar}, representing the power radiated into space, and a loss resistance R_{al}, representing ohmic losses. In reception mode, an incoming electromagnetic wave induces an open-circuit voltage V_{oc} at the antenna's terminals, which then delivers a signal to the receiver's load impedance Z_L.

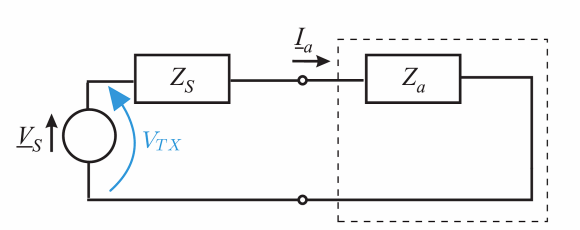

(a) Transmit antenna equivalent circuit, showing the source voltage V_S, source impedance Z_S, transmit voltage V_{TX}, and antenna current I_a.

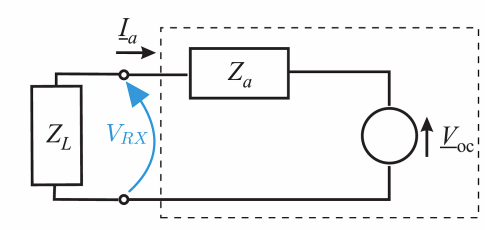

(b) Receive antenna equivalent circuit, showing the induced open-circuit voltage V_{oc}, the load impedance Z_L, and the received voltage V_{RX}.

Figure 1.1: Equivalent circuits for the transmit and receive antennas

The equivalent circuits for the transmitter and receiver are drawn in Figure 1.1. In Figure 1.1a, can be seen the equivalent circuit of the transmitter. The voltage source V_S with its internal impedance Z_S drives the antenna, resulting in a current I_a and a voltage V_{TX} at the antenna's input terminals. At the receiver (Figure 1.1b), the incoming wave induces an open-circuit voltage V_{oc}, which in turn produces the received voltage V_{RX} across the load impedance Z_L.

For this project, it was considered that the electronics are perfectly matched to the antennas. This implies that for the transmitter, the source impedance is the complex conjugate of the antenna impedance:

$$Z_S = Z_a^* \tag{1.1}$$

and for the receiver, the load impedance is the complex conjugate of the antenna impedance:

$$Z_L = Z_a^* \tag{1.2}$$

This consideration ensures maximum power transfer.

1.1 Antenna Effective Height

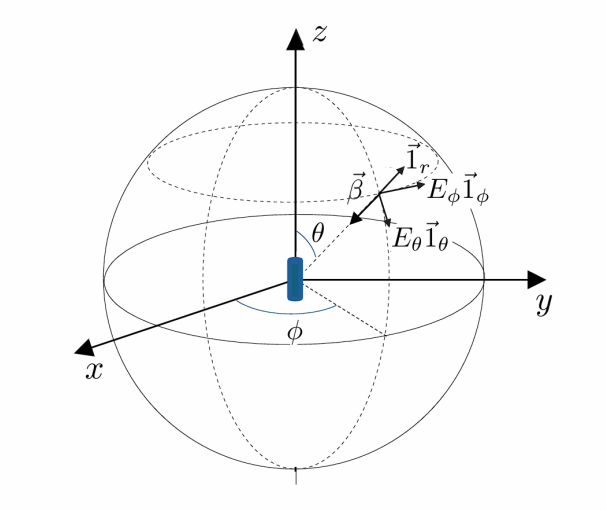

Figure 1.2: Illustration of the vertical dipole antenna and coordinate axes.

The effective height $\vec{h}_e$ of an antenna links the circuit domain to the electromagnetic wave domain. It is derived from the current distribution $\vec{J}(\vec{r}\,')$ on the antenna when transmitting with an input current $\underline{I}_a$:

$$\vec{h}_e(\theta,\phi) = \frac{1}{\underline{I}_a}\int_{\mathcal{D}} \vec{J}(\vec{r}\,')e^{j\beta(\vec{r}\,'\cdot\vec{1}_r)}dV' \tag{1.3}$$

where $\mathcal{D}$ is the volume of the antenna, $\vec{1}_r$ is the unit vector in the direction of radiation (θ,ϕ), and β is the wavenumber:

$$\beta = \frac{2\pi}{\lambda} \tag{1.4}$$

For a thin, vertical half-wave dipole antenna of length $L = \frac{\lambda}{2}$ oriented along the z-axis and centered at the origin (Figure 1.2), the current flows only in the z-direction. The current distribution is given by:

$$\vec{J}(\vec{r}\,') = \underline{I}_a \cos(\beta z')\delta(x')\delta(y')\vec{1}_z, \quad \text{for } -\frac{\lambda}{4} \le z' \le \frac{\lambda}{4} \tag{1.5}$$

where $\delta(x')$ and $\delta(y')$ are Dirac's deltas.

The volume integral reduces to a line integral along the z-axis. The dot product in the exponent simplifies to:

$$\vec{r}\,' \cdot \vec{1}_r = z'\cos\theta \tag{1.6}$$

Substituting this into Equation 1.3 gives:

$$\vec{h}_e(\theta,\phi) = \left(\int_{-\frac{\lambda}{4}}^{\frac{\lambda}{4}} \cos(\beta z')e^{j\beta z'\cos\theta}dz'\right)\vec{1}_z \tag{1.7}$$

The integral in Equation 1.7 is solved using Euler's formula:

$$\cos(\beta z') = \frac{1}{2}(e^{j\beta z'} + e^{-j\beta z'}) \tag{1.8}$$

$$\int_{-\frac{\lambda}{4}}^{\frac{\lambda}{4}} \cos(\beta z') e^{j\beta z' \cos\theta} dz' = \frac{1}{2} \int_{-\frac{\lambda}{4}}^{\frac{\lambda}{4}} \left(e^{j\beta z'(1+\cos\theta)} + e^{j\beta z'(\cos\theta - 1)} \right) dz' \tag{1.9}$$

$$= \frac{1}{2j\beta} \left[\frac{e^{j\beta z'(1+\cos\theta)}}{1+\cos\theta} + \frac{e^{j\beta z'(\cos\theta-1)}}{\cos\theta - 1} \right]_{-\frac{\lambda}{4}}^{\frac{\lambda}{4}} \tag{1.10}$$

With $\beta = \frac{2\pi}{\lambda}$, the term $\frac{\beta\lambda}{4}$ simplifies to $\frac{\pi}{2}$. Evaluating at the limits yields:

$$= \frac{1}{2j\beta} \left[\frac{e^{j\frac{\pi}{2}(1+\cos\theta)} - e^{-j\frac{\pi}{2}(1+\cos\theta)}}{1+\cos\theta} - \frac{e^{j\frac{\pi}{2}(1-\cos\theta)} - e^{-j\frac{\pi}{2}(1-\cos\theta)}}{1-\cos\theta} \right] \tag{1.11}$$

Using the definition of sine: $\sin(x) = \frac{e^{jx} - e^{-jx}}{2j}$

$$= \frac{1}{\beta} \left[\frac{\sin\left(\frac{\pi}{2}(1+\cos\theta)\right)}{1+\cos\theta} - \frac{\sin\left(\frac{\pi}{2}(\cos\theta - 1)\right)}{1-\cos\theta} \right] \tag{1.12}$$

$$= \frac{1}{\beta} \left[\frac{\sin(\frac{\pi}{2} + \frac{\pi}{2}\cos\theta)}{1+\cos\theta} + \frac{\sin(\frac{\pi}{2} - \frac{\pi}{2}\cos\theta)}{1-\cos\theta} \right] \tag{1.13}$$

Applying the identities $\sin(\frac{\pi}{2} + x) = \cos(x)$ and $\sin(\frac{\pi}{2} - x) = \cos(x)$:

$$= \frac{1}{\beta} \left[\frac{\cos(\frac{\pi}{2}\cos\theta)}{1+\cos\theta} + \frac{\cos(\frac{\pi}{2}\cos\theta)}{1-\cos\theta} \right] \tag{1.14}$$

$$= \frac{\cos(\frac{\pi}{2}\cos\theta)}{\beta} \left[\frac{(1-\cos\theta) + (1+\cos\theta)}{(1+\cos\theta)(1-\cos\theta)} \right] = \frac{2\cos(\frac{\pi}{2}\cos\theta)}{\beta \sin^2\theta} \tag{1.15}$$

Substituting $\beta = \frac{2\pi}{\lambda}$, the final result of the integral is:

$$\frac{\lambda}{\pi} \frac{\cos(\frac{\pi}{2}\cos\theta)}{\sin^2\theta} \tag{1.16}$$

The effective height for the vertical half-wave dipole is therefore:

$$\vec{h}_e(\theta, \phi) = \frac{\lambda}{\pi} \frac{\cos(\frac{\pi}{2}\cos\theta)}{\sin^2\theta} \vec{1}_z \tag{1.17}$$

This vector is oriented along the z-axis. For reception, the induced voltage depends on the

component of the effective height that is transverse to the direction of wave propagation, $\vec{1}_r$. This transverse component is denoted $\vec{h}_{e\perp}$. The unit vector $\vec{1}_z$ is expressed in spherical coordinates as:

$$\vec{1}_z = \cos\theta\vec{1}_r - \sin\theta\vec{1}_\theta \tag{1.18}$$

The transverse part, $\vec{h}_{e\perp}$, consists of the components in the $\vec{1}_\theta$ and $\vec{1}_\phi$ directions. Substituting the spherical representation of $\vec{1}_z$ into Equation (1.17) and retaining only the transverse component gives:

$$\vec{h}_{e\perp}(\theta,\phi) = -\frac{\lambda}{\pi}\frac{\cos(\frac{\pi}{2}\cos\theta)}{\sin^2\theta}(\sin\theta\vec{1}_\theta) = -\frac{\lambda}{\pi}\frac{\cos(\frac{\pi}{2}\cos\theta)}{\sin\theta}\vec{1}_\theta \tag{1.19}$$

This is the general expression for the transverse effective height of a vertical $\frac{\lambda}{2}$ dipole. In the horizontal plane, where $\theta = \frac{\pi}{2}$, the expression simplifies significantly. The transverse effective height in the horizontal plane is therefore:

$$\boxed{\vec{h}_{e\perp}\left(\theta = \frac{\pi}{2}, \phi\right) = -\frac{\lambda}{\pi}\vec{1}_\theta} \tag{1.20}$$

This final expression indicates that in the horizontal plane, the antenna's effective height has a constant magnitude of $\frac{\lambda}{\pi}$, is constant for all ϕ, and is oriented in the $\vec{1}_\theta$ direction. This means that the Gain of the this antenna is constant along the .....

1.2 Emitted Electric Field in Free-Space

The electric field radiated by an antenna is given by:

$$\underline{\vec{E}}(\vec{r}) = -j\omega\underline{I}_a\frac{\mu_0}{4\pi}\frac{e^{-j\beta r}}{r}\vec{h}_{e\perp}(\theta,\phi) \tag{1.21}$$

Substituting the transverse effective height for the horizontal plane found in Equation (1.20) into the general expression gives:

$$\underline{\vec{E}}(r,\frac{\pi}{2},\phi) = -j\omega\underline{I}_a\frac{\mu_0}{4\pi}\frac{e^{-j\beta r}}{r}\left(-\frac{\lambda}{\pi}\vec{1}_\theta\right) = j\underline{I}_a\frac{\omega\mu_0\lambda}{4\pi^2}\frac{e^{-j\beta r}}{r}\vec{1}_\theta \tag{1.22}$$

Expressing this field in terms of circuit parameters involves the substitutions $\omega = 2\pi f_c$, $\lambda = \frac{c}{f_c}$, $\mu_0 = \frac{Z_0}{c}$, and propagation delay $\tau = \frac{r}{c}$. The exponential term becomes:

$$e^{-j\beta r} = e^{-j\frac{2\pi}{\lambda}c\tau} = e^{-j2\pi f_c\tau} \tag{1.23}$$

The electric field is then:

$$\underline{\vec{E}} = j\underline{I}_a\frac{(2\pi f_c)(\frac{Z_0}{c})(\frac{c}{f_c})}{4\pi^2}\frac{e^{-j2\pi f_c\tau}}{c\tau}\vec{1}_\theta = j\underline{I}_a\frac{Z_0}{2\pi c\tau}e^{-j2\pi f_c\tau}\vec{1}_\theta \tag{1.24}$$

A half-wave dipole at its resonant frequency has an almost purely real impedance, meaning its reactance is negligible ($X_a \approx 0$), so $Z_a = R_a + jX_a \approx R_a$. Under the perfect matching condition ($Z_S = Z_a^*$), the total impedance in the transmitter circuit is $Z_S + Z_a \approx Z_a^* + Z_a \approx 2R_a$. The antenna current is then related to the transmit voltage by Ohm's law:

$$\underline{I}_a = \frac{\underline{V}_{TX}}{2R_a} \tag{1.25}$$

Substituting $\underline{I}_a$ in Equation (1.24):

$$\boxed{\underline{\vec{E}} = j\frac{Z_0}{4\pi R_a c\tau}\underline{V}_{TX}e^{-j2\pi f_c \tau}\vec{1}_\theta} \tag{1.26}$$

1.3 Received Voltage in Free-Space

The open-circuit voltage $\underline{V}_{oc}$ induced at the terminals of a receiving antenna is given by the dot product of its effective height and the incident electric field:

$$\underline{V}_{oc} = -\vec{h}_{e\perp}^{RX} \cdot \underline{\vec{E}} \tag{1.27}$$

The receiving antenna is also a vertical $\frac{\lambda}{2}$ dipole, so its transverse effective height in the horizontal plane is given by Equation (1.20). The incident electric field is given by Equation (1.26). The dot product is:

$$\underline{V}_{oc} = -\left(-\frac{\lambda}{\pi}\vec{1}_\theta\right) \cdot \left(j\frac{Z_0}{4\pi R_a c\tau}\underline{V}_{TX}e^{-j2\pi f_c \tau}\vec{1}_\theta\right) \tag{1.28}$$

$$= j\frac{\lambda Z_0}{4\pi^2 R_a c\tau}\underline{V}_{TX}e^{-j2\pi f_c \tau} \tag{1.29}$$

The voltage $\underline{V}_{RX}$ across the receiver load Z_L is found using a voltage divider on the receiver equivalent circuit (Figure 1.1b):

$$\underline{V}_{RX} = \underline{V}_{oc}\frac{Z_L}{Z_a + Z_L} \tag{1.30}$$

With perfect matching ($Z_L = Z_a^*$) and a resonant dipole ($Z_a \approx R_a$), the total impedance in the receiver circuit is $Z_a + Z_L \approx R_a + R_a = 2R_a$. The expression for $\underline{V}_{RX}$ simplifies to:

$$\underline{V}_{RX} \approx \frac{\underline{V}_{oc}}{2} \tag{1.31}$$

Substituting the expression for $\underline{V}_{oc}$ gives the final relationship between the received and transmitted voltages:

$$\boxed{\underline{V}_{RX} = j\frac{\lambda Z_0}{8\pi^2 R_a c\tau}\underline{V}_{TX}e^{-j2\pi f_c \tau}} \tag{1.32}$$

2

Line-of-Sight Channel - Narrowband Analysis

The analysis begins with the simplest communication scenario: a direct Line-of-Sight ray between the transmitter TX and the receiver RX. A narrowband analysis is conducted, which assumes that the signal's bandwidth is much smaller than the channel's coherence bandwidth. This simplification allows the channel to be characterized by one complex coefficient.

The physical channel can be described by its time-variant impulse response, which for a set of N multiray components is:

$$h(\tau, t) = \sum_{n=1}^{N} \alpha_n(t)\delta(\tau - \tau_n) \tag{2.1}$$

where $\alpha_n(t)$ and τ_n are the complex amplitude and propagation delay of the n-th ray, respectively.

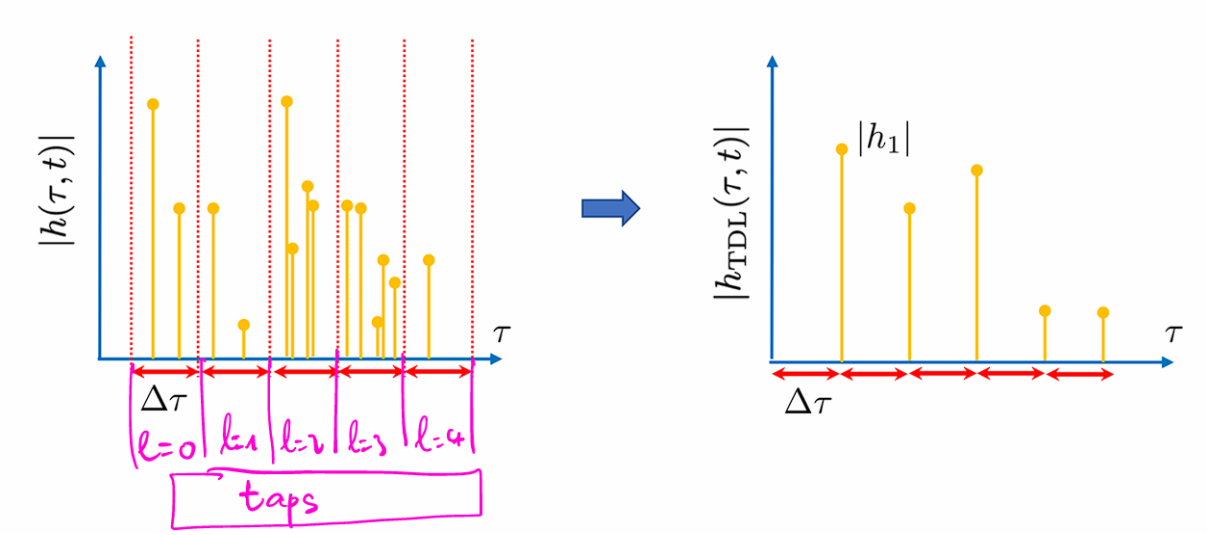

Figure 2.1: Physical impulse response and TDL model under the Uncorrelated Scattering assumption[1]

A practical communication system has a finite bandwidth B, which limits its ability to resolve rays arriving at different times. The system's time resolution is $\Delta\tau = 1/B$.

[1]The US assumption posits that the complex amplitudes of multipath components arriving at different delays are statistically uncorrelated, meaning they are independent from one another

The received signal is defined by:

$$y(t) = \sum_{l} x(t - l\Delta\tau) \underbrace{\int_{0}^{\infty} h(\tau, t)\,\mathrm{sinc}(B(\tau - l\Delta\tau))d\tau}_{h_l(t)} \tag{2.2}$$

From there, can be defined the complex gain of the l-th tap:

$$h_l(t) = \int_{0}^{\infty} h(\tau, t)\,\mathrm{sinc}(B(\tau - l\Delta\tau))d\tau \tag{2.3}$$

$$= \int_{0}^{\infty} (\sum_{n=1}^{N} \alpha_n(t)\delta(\tau - \tau_n)) \cdot \mathrm{sinc}(B(\tau - l\Delta\tau))d\tau \tag{2.4}$$

$$= \sum_{n=1}^{N} \alpha_n(t)\,\mathrm{sinc}\left(B\left(\tau_n - l\Delta\tau\right)\right) \tag{2.5}$$

$$\implies \boxed{h_l(t) \approx \sum_{\tau_n \in \mathrm{tap}\, l} \alpha_n(t)} \tag{2.6}$$

Equation (2.6) can be written because sinc(.) maximizes the amplitude of the components of the l-th tap, and the components of other taps are drastically attenuated. The components of the l-th tap appear not to be delayed between one another.

The physical limitation of the finite bandwidth of the system leads to the Tapped Delay Line model. The impulse response of the TDL model is a discrete-time representation of the physical channel as shown in Figure 2.1:

$$h_{TDL}(\tau, t) = \sum_{l=0}^{L} h_l(t)\delta(\tau - l\Delta\tau) \tag{2.7}$$

The condition for a narrowband channel is that the signal bandwidth B is much smaller than the channel's coherence bandwidth Δf_c. The coherence bandwidth is inversely proportional to the channel's delay spread, $\sigma_\tau = max|\tau_i - \tau_j|$, which is the maximum delay that exist between two consecutive rays. The narrowband condition is thus expressed as:

$$B \ll \Delta f_c \approx \frac{1}{\sigma_\tau} \implies \Delta\tau \gg \sigma_\tau \tag{2.8}$$

This inequality means the system's time resolution is much larger than the delay spread. From the receiver's perspective, all MPCs arrive at effectively the same time. Consequently, all MPCs fall into the first tap ($l = 0$) of the TDL model. The summation in Equation (2.7) therefore reduces to one term for $l = 0$:

$$h_{TDL}(\tau, t) = h_0(t)\delta(\tau) \tag{2.9}$$

where the tap gain $h_0(t)$ is the sum of all individual ray gains:

$$\boxed{h_0(t) = \sum_{n=1}^{N} \alpha_n(t)} \quad N \text{ being the total number of MPCs} \tag{2.10}$$

2.1 Antenna Gain

The gain of an antenna, $G(\theta, \phi)$, quantifies its ability to concentrate radiated power in a specific direction. It is defined as:

$$G(\theta, \phi) = \frac{\pi Z_0}{R_a} \frac{|\vec{h}_{e\perp}(\theta, \phi)|^2}{\lambda^2} \tag{2.11}$$

where Z_0 is the impedance of free space, R_a is the antenna's radiation resistance, λ is the wavelength, and $\vec{h}_{e\perp}(\theta, \phi)$ is the transverse component of the antenna's effective height.

As derived earlier (Equation 1.20), the transverse effective height for a vertical half-wave dipole in the horizontal plane ($\theta = \frac{\pi}{2}$) is:

$$\vec{h}_{e\perp}\left(\frac{\pi}{2}, \phi\right) = -\frac{\lambda}{\pi}\vec{1}_\theta \tag{2.12}$$

The magnitude squared of this vector is therefore:

$$\left|\vec{h}_{e\perp}\left(\frac{\pi}{2}, \phi\right)\right|^2 = \left|-\frac{\lambda}{\pi}\vec{1}_\theta\right|^2 = \frac{\lambda^2}{\pi^2} \tag{2.13}$$

Substituting this result into the general gain Equation (2.11) provides the expression for the gain of a lossless half-wave dipole in the horizontal plane:

$$G = G\left(\frac{\pi}{2}, \phi\right) = \frac{\pi Z_0}{R_a} \frac{1}{\lambda^2} \left(\frac{\lambda^2}{\pi^2}\right) = \frac{\pi Z_0 \lambda^2}{\pi^2 R_a \lambda^2} \tag{2.14}$$

Simplifying this expression yields the final result:

$$G = \frac{Z_0}{\pi R_a} \tag{2.15}$$

2.2 Impulse Response $h(\tau)$

For a single, time-invariant Line-of-Sight ray, the channel impulse response is characterized by a single complex amplitude, α_1, and a propagation delay, τ_1. The impulse response is thus expressed as:

$$h(\tau) = \alpha_1 \delta(\tau - \tau_1) \tag{2.16}$$

The complex amplitude α_1 has to be determined. This can be achieved by relating the circuit-level voltages at the transmitter and receiver. The relationship between the transmitted power

P_{TX} and the received power P_{RX} is defined by the squared magnitude of the complex amplitude:

$$P_{RX} = |\alpha_1|^2 P_{TX} \tag{2.17}$$

The transmitted and received powers can be expressed in terms of the terminal voltages $\underline{V}_{TX}$ and $\underline{V}_{RX}$ and the antenna radiation resistance R_a, assuming perfectly matched conditions:

$$P_{TX} = \frac{1}{2} R_a |\underline{I}_a|^2 = \frac{1}{2} R_a \frac{|\underline{V}_{TX}|^2}{4R_a^2} = \frac{|\underline{V}_{TX}|^2}{8R_a} \tag{2.18}$$

$$P_{RX} = \frac{1}{2} R_a |\underline{I}_a|^2 = \frac{1}{2} R_a \frac{|\underline{V}_{RX}|^2}{R_a^2} = \frac{|\underline{V}_{RX}|^2}{2R_a} \tag{2.19}$$

Substituting these power definitions into the power relationship gives:

$$\frac{|\underline{V}_{RX}|^2}{2R_a} = |\alpha_1|^2 \frac{|\underline{V}_{TX}|^2}{8R_a} \tag{2.20}$$

Solving for $|\alpha_1|^2$ yields:

$$|\alpha_1|^2 = \frac{8R_a}{2R_a} \frac{|\underline{V}_{RX}|^2}{|\underline{V}_{TX}|^2} = 4 \frac{|\underline{V}_{RX}|^2}{|\underline{V}_{TX}|^2} \tag{2.21}$$

This implies a relationship between the magnitudes: $|\alpha_1| = 2\frac{|\underline{V}_{RX}|}{|\underline{V}_{TX}|}$. This motivates defining the complex amplitude α_1 directly from the complex voltage ratio:

$$\alpha_1 = 2 \frac{\underline{V}_{RX}}{\underline{V}_{TX}} \tag{2.22}$$

The relationship between the received and transmitted voltages for a free-space LOS ray was derived previously in Equation (1.32) as:

$$\underline{V}_{RX} = j \frac{\lambda Z_0}{8\pi^2 R_a c \tau_1} \underline{V}_{TX} e^{-j2\pi f_c \tau_1} \tag{2.23}$$

Substituting this into Equation (2.22) gives the expression for α_1:

$$\alpha_1 = 2 \left(j \frac{\lambda Z_0}{8\pi^2 R_a c \tau_1} e^{-j2\pi f_c \tau_1} \right) = j \frac{\lambda Z_0}{4\pi^2 R_a c \tau_1} e^{-j2\pi f_c \tau_1} \tag{2.24}$$

Replacing the product of the speed of light c and the delay τ_1 with the distance $d_1 = c\tau_1$, the complex amplitude is:

$$\alpha_1 = j \frac{\lambda Z_0}{4\pi^2 R_a d_1} e^{-j2\pi f_c \tau_1} \tag{2.25}$$

The channel impulse response for the LOS ray is therefore:

$$\boxed{h(\tau) = \left(j \frac{\lambda Z_0}{4\pi^2 R_a d_1} e^{-j2\pi f_c \tau_1} \right) \delta(\tau - \tau_1)} \tag{2.26}$$

where $\tau_1 = d_1/c$.

2.3 Transfer Function $H(f)$

The transfer function $H(f)$ is obtained by taking the Fourier transform of the impulse response $h(\tau)$:

$$H(f) = \mathcal{FT}\{h(\tau)\} = \int_{-\infty}^{\infty} h(\tau)e^{-j2\pi f\tau}d\tau = \int_{-\infty}^{\infty} \left(\alpha_1\delta(\tau-\tau_1)\right)e^{-j2\pi f\tau}d\tau \tag{2.27}$$

Applying the sifting property of the Dirac delta function, which states that $\int g(x)\delta(x-a)dx = g(a)$, the integral simplifies to:

$$H(f) = \alpha_1 e^{-j2\pi f\tau_1} \tag{2.28}$$

Substituting the derived expression for α_1 from Equation (2.25):

$$H(f) = \left(j\frac{\lambda Z_0}{4\pi^2 R_a d_1}e^{-j2\pi f_c\tau_1}\right)e^{-j2\pi f\tau_1} \tag{2.29}$$

$$\Rightarrow \boxed{H(f) = j\frac{\lambda Z_0}{4\pi^2 R_a d_1}e^{-j2\pi(f_c+f)\tau_1}} \tag{2.30}$$

This function shows that the channel introduces a phase shift that is linear with the baseband frequency f, which corresponds to the time delay τ_1. The magnitude $|H(f)|$ is constant across all frequencies.

2.4 Narrowband Transfer Function h_{NB}

As said in Equation (2.9), the narrowband is defined such that all MPCs fall into a single tap:

$$h_{NB} = \mathcal{FT}\{h_{TDL}(t,\tau)\} = \mathcal{FT}\{h_0(t)\delta(\tau)\} \tag{2.31}$$

$$= \int_{-\infty}^{\infty} h_0(t)e^{-j2\pi f\tau}\delta(\tau)d\tau \tag{2.32}$$

$$= h_0(t)e^{-j2\pi f\cdot 0} \tag{2.33}$$

$$\Longrightarrow \boxed{h_{NB} = h_0(t)} \tag{2.34}$$

As found in Equation (2.10), for a single LOS ray, the narrowband channel transfer function is equal to the complex amplitude α_1:

$$h_{NB} = \sum_{n=1}^{N=1}\alpha_n(t) = \alpha_1 \tag{2.35}$$

Using the result from Equation (2.25), the narrowband transfer function is:

$$\boxed{h_{NB} = j\frac{\lambda Z_0}{4\pi^2 R_a d_1}e^{-j2\pi f_c\tau_1}} \tag{2.36}$$

The LOS channel is thus represented by one complex number, which scales and rotates the transmitted signal.

2.5 Received Power P_{RX}

The received power can now be calculated using the derived complex amplitude α_1 and its relationship to the power gain, $P_{RX} = |\alpha_1|^2 P_{TX}$. First, the magnitude squared of α_1 is computed:

$$|\alpha_1|^2 = \left| j\frac{\lambda Z_0}{4\pi^2 R_a d_1} e^{-j2\pi f_c \tau_1} \right|^2 = \left(\frac{\lambda Z_0}{4\pi^2 R_a d_1} \right)^2 \tag{2.37}$$

Substituting this into the power equation gives the received power as a function of the transmitted power:

$$\boxed{P_{RX} = \left(\frac{\lambda Z_0}{4\pi^2 R_a d_1} \right)^2 P_{TX}} \tag{2.38}$$

To demonstrate that this result is equivalent to the Friis formula, the terms are rearranged. The expression is factored to isolate terms corresponding to the antenna gains:

$$P_{RX} = \frac{\lambda^2 Z_0^2}{16\pi^4 R_a^2 d_1^2} P_{TX} \tag{2.39}$$

$$= \left(\frac{Z_0^2}{\pi^2 R_a^2} \right) \left(\frac{\lambda^2}{16\pi^2 d_1^2} \right) P_{TX} \tag{2.40}$$

$$= \left(\frac{Z_0}{\pi R_a} \right) \left(\frac{Z_0}{\pi R_a} \right) \left(\frac{\lambda}{4\pi d_1} \right)^2 P_{TX} \tag{2.41}$$

Using the expression for the gain of a lossless half-wave dipole in the horizontal plane as derived in Equation (2.15), $G = Z_0/(\pi R_a)$, and assuming identical transmit and receive antennas ($G_{TX} = G_{RX} = G$):

$$P_{RX} = G_{TX} G_{RX} \left(\frac{\lambda}{4\pi d_1} \right)^2 P_{TX} \tag{2.42}$$

This result is identical to the Friis transmission formula. This validates the entire derivation, confirming that the complex amplitude α_1 derived from the voltage ratio correctly predicts the power relationship under free-space LOS conditions.

2.6 Interpretation of Results

The derivations confirm the principles of a simple LOS communication link.

- **Frequency-Flat Channel:** The single propagation ray results in a transfer function $|H(f)|$ that is constant with frequency. This means the channel does not distort the signal's spectrum, illustrating flat fading. This is a direct consequence of having no time dispersion, meaning zero delay spread).
- **Validation of Friis' Formula:** The derivation, starting from the circuit-level voltage

relationship to find the complex amplitude α_1, and then using it to find the received power, shows a result identical to the Friis' formula.

3

Full Channel, Narrowband Analysis

The analysis now expands from the LOS model to a full-channel model. This section considers the impact of multiray components generated by reflections off the buildings lining. The analysis remains within the narrowband assumption, where the channel's response can be characterized by a single complex coefficient, but this coefficient now incorporates the vector sum of all significant propagation rays, not just the LOS.

In a realistic urban environment, the signal transmitted from TX to RX does not travel along a single ray. Instead, it propagates along multiple rays due to reflections from surrounding objects, in this case, the building facades. Each of these rays is an MPC. The total received signal is the vector sum of all these MPCs. The narrowband channel transfer function, previously represented by a single complex gain α_1 for the LOS ray, is now the sum of the complex gains of all MPCs:

$$h_{NB} = \sum_{n=1}^{N} \alpha_n \tag{3.1}$$

where N is the total number of MPCs, including the LOS ray and all reflected rays. Each complex gain α_n is a function of the ray's length, the reflection coefficients of the surfaces it interacts with, and the propagation delay.

The primary tool for identifying these rays and calculating their geometry is the image method. For each reflecting surface, an image of the transmitter is created. A straight line from this image to the receiver identifies the ray of the reflected wave, as shown in Figure 3.1. This method can be extended recursively to find rays with multiple reflections.

3.1 Multiray Component Geometry

To find the paths of all significant rays, the image method is used. The scenario is a urban street of width $2w = 20$ m. The transmitter TX and receiver RX are placed symmetrically in the center of the street, separated by a distance d. The building walls are represented by two parallel lines at $y = w$ and $y = -w$.

LOS ray

The LOS ray is the direct and unobstructed path between the transmitter and receiver. It is considered as the first path component, meaning $n = 1$.

- **Path Length:** $d_1 = d$ The

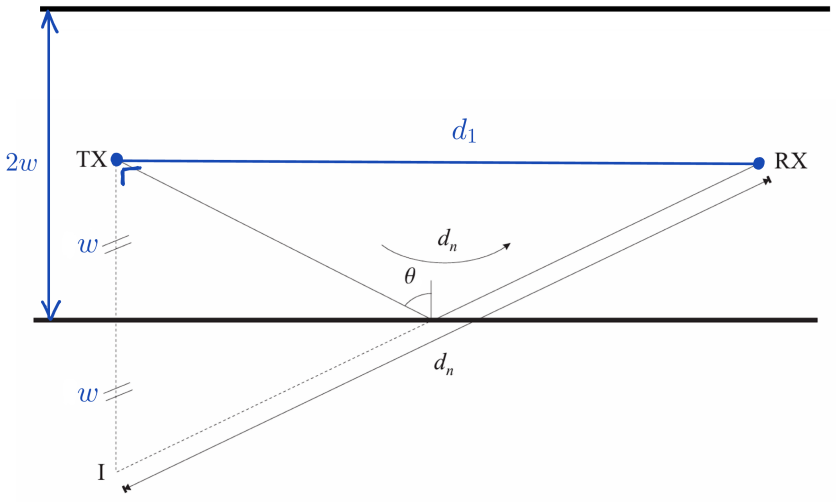

Figure 3.1: The image method for a single reflection. The ray of the reflected ray from TX to RX is found by drawing a straight line from the image transmitter I to RX.

- **Propagation Delay:**

$$\tau_1 = \frac{d}{c} \tag{3.2}$$

Single Reflection rays

There are two distinct paths involving one reflection, one from the top wall and one from the bottom wall. Using the image method, we create a virtual source I_1 by reflecting the TX across the wall. The path length is the straight-line distance from I_1 to the RX.

- **Path Length:** The geometry forms a right triangle with legs and d and $2w$ (the vertical distance between the image and the RX).

$$d_n = \sqrt{d^2 + (2w)^2} \tag{3.3}$$

- **Propagation Delay:**

$$\tau_n = \frac{\sqrt{d^2 + (2w)^2}}{c} \tag{3.4}$$

- **Angle of Incidence:** The angle of incidence with the wall is given by:

$$\sin(\theta_n) = \frac{d}{d_n} \tag{3.5}$$

Double Reflection rays

There are two paths involving two reflections (for example: Wall 1 $\rightarrow$ Wall 2 $\rightarrow$ RX). To find the path length, we create a second-order image I_2, by reflecting the first-order image I_1 across the opposite wall.

- **Path Length:** The vertical separation between the second-order image I_2 and the RX is

now $4w$.

$$d_n = \sqrt{d^2 + (4w)^2} \tag{3.6}$$

- **Propagation Delay:**

$$\tau_n = \frac{\sqrt{d^2 + (4w)^2}}{c} \tag{3.7}$$

- **Angle of Incidence:** The angle of incidence is the same for both reflections and is given by:

$$\cos(\theta_n) = \frac{d}{d_n} = \frac{d}{\sqrt{d^2 + (4w)^2}} \tag{3.8}$$

K-th Order Reflection Rays (Recursive Approach)

While closed-form expressions can be derived for this simple geometry, a more robust and general method is to define the process recursively, as implemented in the simulation. To find all paths with up to K reflections, the algorithm extends the image method by systematically generating and validating potential ray paths.

Code Implementation :

The process is coded using a recursive function `findReflectedRaysRecursive`, which builds a tree of image sources as illustrated in Figure 3.2. The function starts with the real transmitter (the 0-order source) and the desired number of reflections. In each recursive step, it mirrors the current source across every wall in the environment using `findSymmetricAcrossLine` function, creating a new set of higher-order image sources. It then calls itself for each new image, with the remaining number of reflections decremented. To avoid physically redundant paths, a source is never immediately reflected back across the same wall it was just generated from.

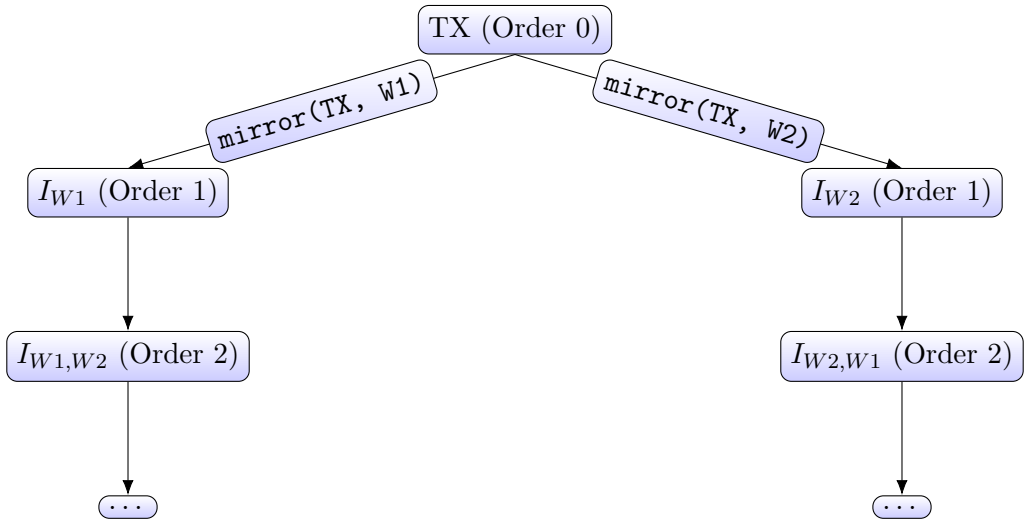

Figure 3.2: Conceptual tree of image sources generated by `findReflectedRaysRecursive`. Each level corresponds to an order of reflection.

The recursion stops when the desired reflection order is reached. At this point, the sequence of

image sources defines a potential ray path. However, this path is only geometrically hypothetical. It must be validated by the `validateRayPath` function, which traces the path backward from RX to TX. The logic of this validation is detailed in the flowchart in Figure 3.3.

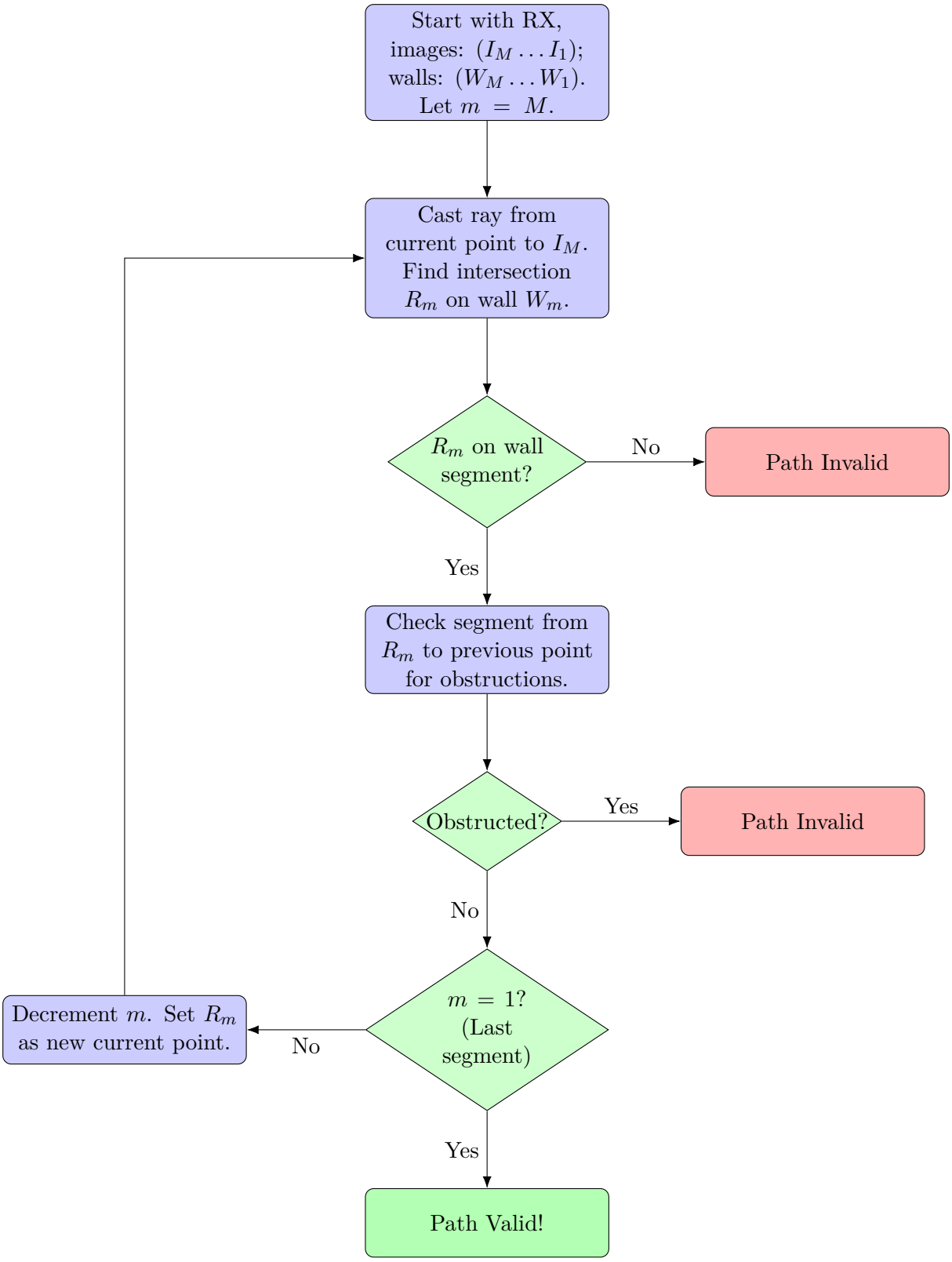

Figure 3.3: Flowchart of the backward path validation process in `validateRayPath` function.

The validation process follows the sequence:

1. Starting from the RX, a line is cast to the final image source (I_M). Its intersection with the corresponding wall segment (W_M) is found using `findSegmentIntersection`. If an intersection point does not exist on the finite wall segment, the path is invalid.

2. If the reflection point is valid, the path segment from it to the RX is checked for obstructions by any other wall. If it is obstructed, the path is invalid.

3. The process is then repeated, tracing backward from the newly found reflection point to the next image in the sequence (I_{K-1}) to find the next reflection point on its respective wall (W_{K-1}).

4. This continues until the entire path has been traced back to the original transmitter. A path is only considered valid if every segment is unobstructed and every reflection point lies on its physical wall.

Once n-th ray path is validated, the function `calculatePhysicalProperties` computes its total path length d_n, by summing the lengths of its segments. It also calculates the angle of incidence for each reflection to find the product of the Fresnel reflection coefficients.

For the specific symmetric geometry of the setup, this recursive algorithm correctly identifies the paths whose lengths are given by the simplified formula:

$$d_n = \sqrt{d^2 + (2Mw)^2} \tag{3.9}$$

The corresponding propagation delay is:

$$\tau_n = \frac{\sqrt{d^2 + (2Mw)^2}}{c} \tag{3.10}$$

An the Angle of incidence is defined by:

$$\cos(\theta_n) = \frac{d}{d_n} = \frac{d}{\sqrt{d^2 + (2Mw)^2}} \tag{3.11}$$

For a simulation considering up to $M = 10$ reflections, this process identifies the LOS ray plus two rays for each reflection order, resulting in a total of $N = 1 + 2 \times 10 = 21$ valid MPCs.

3.2 Total Received Voltage

The complex amplitude α_n for each ray n must account for the path loss and any phase changes from reflections. The general form for the complex amplitude of a ray of length d_n with M reflections is:

$$\alpha_n = \left(j \frac{\lambda Z_0}{4\pi^2 R_a d_n} e^{-j2\pi f_c \tau_n} \right) \times \underbrace{\prod_{m=1}^{M} (\Gamma_{\perp,m}(\theta_n))}_{\Gamma_{\text{tot},n}} \tag{3.12}$$

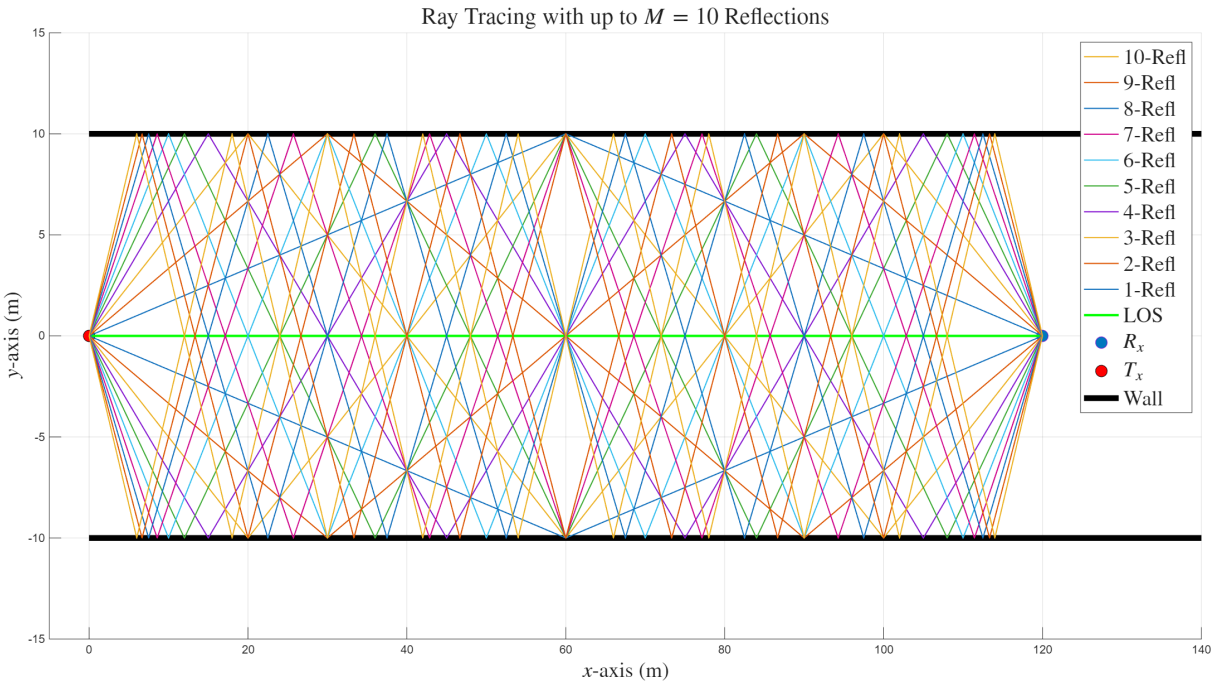

Figure 3.4: Simulation of the image method ray-tracing for 10 reflections, showing the 21 valid MPCs found.

where $\Gamma_{\perp,m}(\theta_n)$ is the reflection coefficient for perpendicular polarization for the n-th MPC at its m-th reflections:

$$\Gamma_{\perp,m}(\theta_n) = \frac{\cos\theta_n - \sqrt{\epsilon_{r,m} - \sin^2\theta_n}}{\cos\theta_n + \sqrt{\epsilon_{r,m} - \sin^2\theta_n}} \tag{3.13}$$

with $\epsilon_{r,m} = 4$ for the buildings. The angle of incidence θ_n is specific to each reflection order.

The narrowband transfer function found in Equation (2.10) is given by :

$$h_{NB} = \sum_{n=1}^{N=7} \alpha_n = \alpha_{LOS} + \sum_{n=2}^{N=7} \alpha_n \tag{3.14}$$

The total received voltage $\underline{V}_{RX}$ is then:

$$\underline{V}_{RX} = \frac{h_{NB}}{2}\underline{V}_{TX} \tag{3.15}$$

3.3 Received Power and Comparison with Friis Formula

The received power is:

$$P_{RX} = |h_{NB}|^2 P_{TX} = \left|\alpha_{LOS} + \sum_{n=2}^{N=7} \alpha_n\right|^2 P_{TX} \tag{3.16}$$

Ray	Type	d_n [m]	τ_n [ns]	θ_n [°]	$\Gamma_{\text{tot},n}$	$\lvert\alpha_n\rvert$	$\arg(\alpha_n)$ [°]
1	LOS	100.00	333.33	0.00	1.00	6.6425×10^{-5}	-150.00
2	1-Ref1	101.98	339.93	78.69	-0.798	5.1961×10^{-5}	48.84
3	1-Ref1	101.98	339.93	78.69	-0.798	5.1961×10^{-5}	48.84
4	2-Ref1	107.70	359.01	68.20	0.427	2.6328×10^{-5}	30.66
5	2-Ref1	107.70	359.01	68.20	0.427	2.6328×10^{-5}	30.66
6	3-Ref1	116.62	388.73	59.04	-0.173	9.8285×10^{-6}	87.21
7	3-Ref1	116.62	388.73	59.04	-0.173	9.8285×10^{-6}	87.21

Table 3.1: Multipath Component Parameters, $M = 3$ reflections, $d = 100$ m

This expression highlights the difference from the LOS only represented by the Friis formula:

$$P_{RX,\text{Friis}} = P_{TX} G_{TX} G_{RX} \left(\frac{\lambda}{4\pi d}\right)^2 = |\alpha_{LOS}|^2 P_{TX} \tag{3.17}$$

The Friis formula represents the power of only the first term ($n = 1$) in the sum. In the full channel model, the total power depends on the vector sum of all 7 MPCs. Because the rays have different lengths d_n and undergo different phase shifts ($e^{-j2\pi f_c \tau_n}$ and from reflections), the complex amplitudes α_n add up coherently.

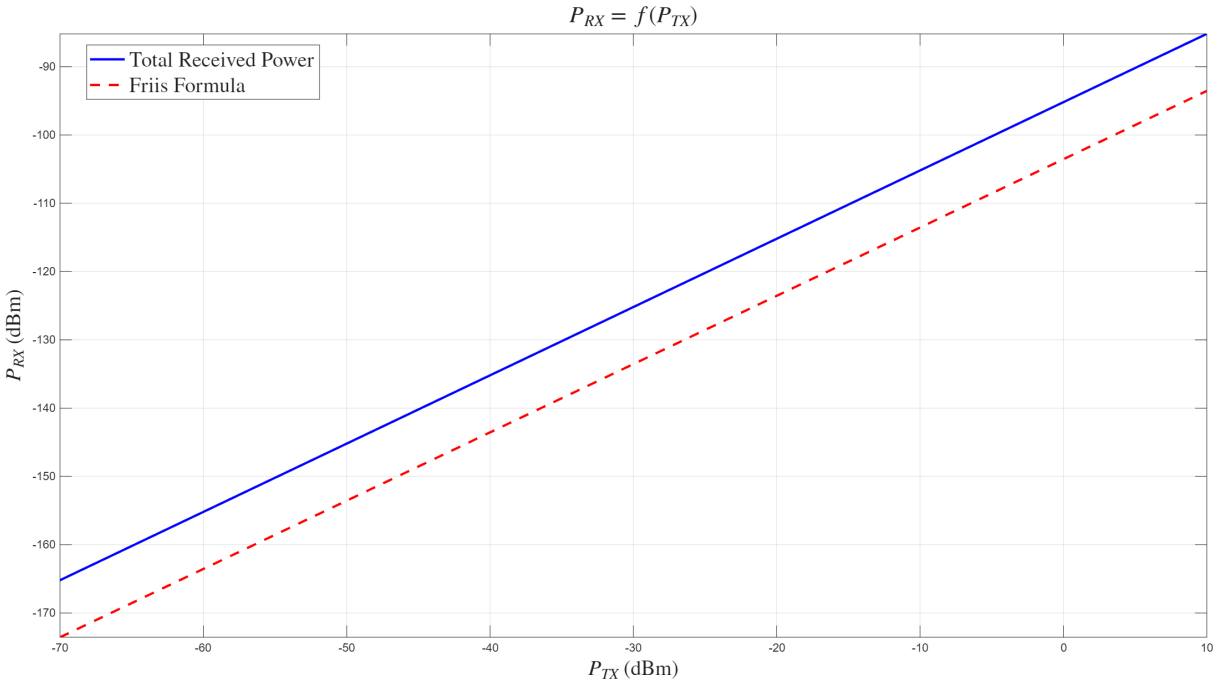

Figure 3.5: Received Power as a function of the Transmitted Power for a fixed channel (d is constant and equal to $1km$). The number of reflections is $M = 10$

This coherent summation results in fast fading for small distances and slow fading for very high distances between TX and RX.
Unlike the monotonic decrease of power with all distances predicted by the Friis formula, the full-channel received power will exhibit significant fluctuations as the distance d changes at smaller distances. As seen in Figure 3.6, for very high values of d, the models gets closer to the Friis formula, because the reflected rays will be drastically attenuated, compared to the LOS ray

- **Constructive Interference:** At locations where the MPCs arrive largely in-phase, their amplitudes add up, resulting in a received power that can be significantly higher than the Friis prediction.
- **Destructive Interference:** At locations where some MPCs arrive out-of-phase, their amplitudes cancel each other out, leading to drops far below the Friis prediction.

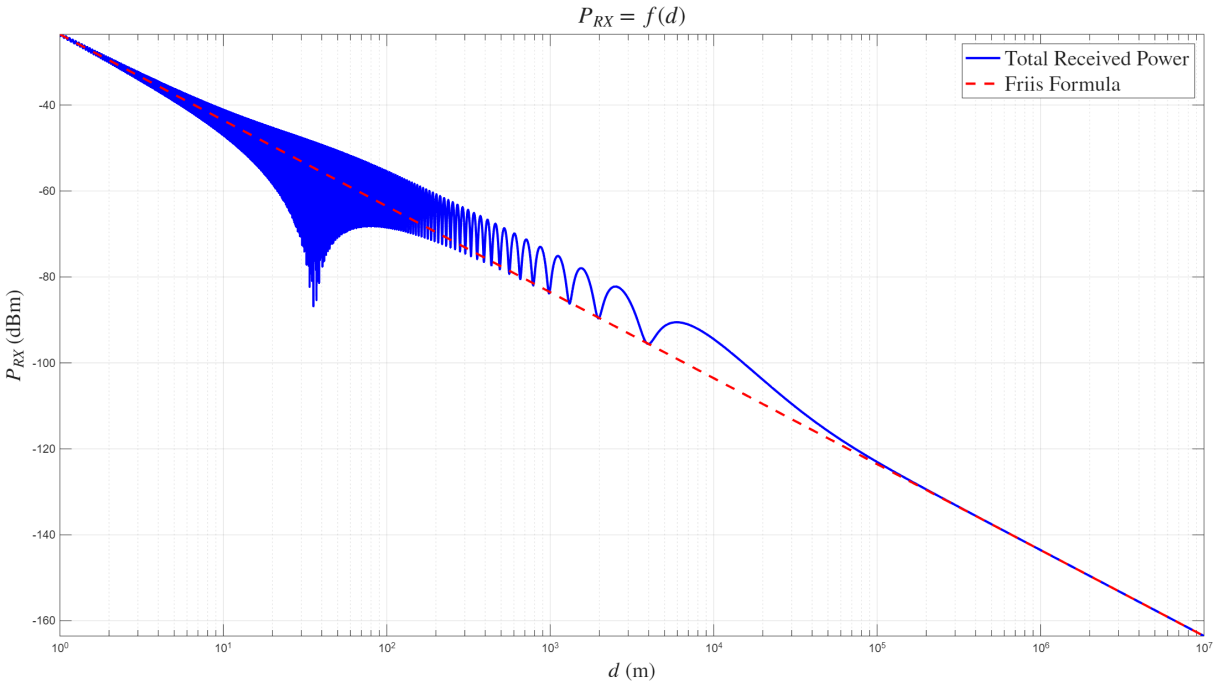

Figure 3.6: Received power as a function of the separation distance between TX and RX in the Multipath Narrow band scenario for $M = 1$ Reflection

3.4 Rician factor

The Rician factor K is a parameter that quantifies the severity of fading in a channel.

$$K = \frac{|\alpha_{LOS}|^2}{\sum_{n=2}^{7} |\alpha_n|^2} = \frac{P_{LOS}}{P_{NLOS}} \tag{3.18}$$

To evaluate this, we need to express $|\alpha_n|^2$ in terms of physical parameters. From the LOS analysis made earlier, we found that the received power for the direct ray is identical to the Friis

formula:

$$P_{LOS} = |\alpha_{LOS}|^2 P_{TX} = G_{TX} G_{RX} \left(\frac{\lambda}{4\pi d}\right)^2 P_{TX} \tag{3.19}$$

This gives us the power gain for the LOS component ($d_1 = d$, $|\Gamma_1|^2 = 1$):

$$|\alpha_{LOS}|^2 = G_{TX} G_{RX} \left(\frac{\lambda}{4\pi d}\right)^2 \tag{3.20}$$

For the n-th MPC that is not the LOS ray, and experiences reflections, the power is reduced by the cumulative reflection coefficient $\Gamma_n = \prod_{m=1}^{M} (\Gamma_{\perp,m}(\theta_n))$. The power gain for a reflected ray of total travel distance d_n is therefore:

$$|\alpha_n|^2 = G_{TX} G_{RX} \left(\frac{\lambda}{4\pi d_n}\right)^2 |\Gamma_n|^2 \tag{3.21}$$

Substituting these expressions for power gain into the K-factor equation:

$$K = \frac{G_{TX} G_{RX} \left(\frac{\lambda}{4\pi d}\right)^2}{\sum_{n=2}^{7} G_{TX} G_{RX} \left(\frac{\lambda}{4\pi d_n}\right)^2 |\Gamma_n|^2} \tag{3.22}$$

The common terms, including antenna gains and wavelength, cancel out, leaving a purely geometric relationship:

$$K = \frac{\frac{1}{d^2}}{\sum_{n=2}^{7} \frac{|\Gamma_n|^2}{d_n^2}} \implies \boxed{K = \frac{1}{d^2 \sum_{n=2}^{7} \frac{|\Gamma_n|^2}{d_n^2}}} \tag{3.23}$$

A high K-factor indicates that the channel is dominated by the LOS ray, and fading will be less severe leading to the Rician distribution. A low K-factor indicates that the NLOS rays are stronger relative to the LOS ray, leading to deep fades characteristic of Rayleigh distribution.

3.5 Path Loss Model

To analyze the large-scale path loss characteristics of the channel, the effects of small-scale fading, which arise from the rapid phase changes of the MPCs, must be averaged out. This is accomplished by computing the local average of the received power, $\langle P_{RX} \rangle$, in 5-meter segments. This spatial averaging smooths out the fast fluctuations, revealing the underlying distance-dependent trend.

The continuous-time definition of this local average at a distance d is given by the integral:

$$\langle P_{RX}(d) \rangle = \frac{1}{5m} \int_{d-2.5m}^{d+2.5m} P_{RX}(x) dx \tag{3.24}$$

In the simulation, where the received power is sampled at discrete points, this integral is approximated by a discrete summation. This is implemented as a moving average filter, which mathematically corresponds to a discrete convolution. The instantaneous power signal, $P_{RX}[i]$, is convolved with a normalized rectangular kernel, $h[k]$, of length $N_{samp,local}$. This length cor-

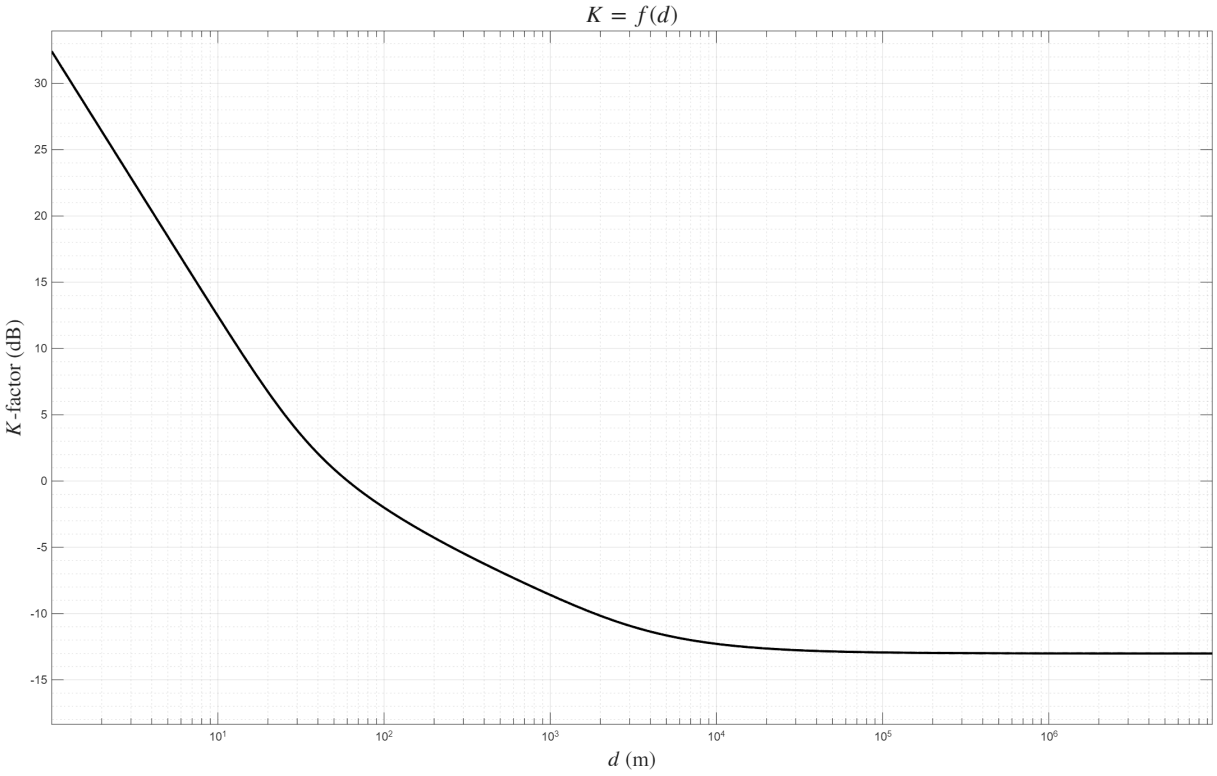

Figure 3.7: K-factor as a function of the separation distance between TX and RX for $K = 10$ reflections

responds to the number of samples within the 5m averaging window. The kernel is defined as:

$$h[k] = \begin{cases} \frac{1}{N_{samp,local}} & \text{for } 0 \leq k < N_{samp,local} \\ 0 & \text{otherwise} \end{cases} \tag{3.25}$$

This corresponds to a vector, $\mathbf{h}$, of $N_{samp,local}$ uniformly weighted coefficients:

$$\mathbf{h} = \frac{1}{N_{samp,local}} \cdot \underbrace{\Big[1, 1, \ldots, 1\Big]}_{N_{samp,local} \text{ elements}} \tag{3.26}$$

The resulting averaged power at sample i, which is the convolution $(P_{RX} * h)[i]$, is then given by:

$$\langle P_{RX}[i] \rangle = \sum_{k=0}^{N_{samp,local}-1} P_{RX}[i-k] \cdot h[k] = \frac{1}{N_{samp,local}} \sum_{k=0}^{N_{samp,local}-1} P_{RX}[i-k] \tag{3.27}$$

$N_{samp,local}$ is defined as:

$$N_{samp} = \text{round}\left(\frac{\text{local window distance}}{\text{sampling distance}}\right) \tag{3.28}$$

The path loss of the channel is defined as $L(d)$ such that:

$$L_{data}(d)[dB] = P_{TX}[dBm] - \langle P_{RX}(d)\rangle[dBm] \tag{3.29}$$

$$= L_{0,data}(d)[dB] - 10\log G_{TX} - 10\log G_{RX} \tag{3.30}$$

Where $L_0(d)$ represent the part of the path loss that does not depend on the antenna. Using Equation (3.29), it can be expressed as:

$$L_{0,data}(d)[dB] = P_{TX}[dBm] + 10\log G_{TX} + 10\log G_{RX} - \langle P_{RX}(d)\rangle[dBm] \tag{3.31}$$

$$= P_{TX}[dBm] + 2 \cdot G_{TX}[dBi] - \langle P_{RX}(d)\rangle[dBm] \tag{3.32}$$

It is empirically proven that in general the path loss model follows the canonical form:

$$L_0(d)[dB] = L_0(d_0) + 10n\log\left(\frac{d}{d_0}\right) \tag{3.33}$$

$$= \underbrace{10n}_{slope}\log(d) + \underbrace{(L_0(d_0) - 10n\log(d_0))}_{intercept} \tag{3.34}$$

Where d_0 is a reference distance, and n is the path loss exponent. This exponent describes how quickly the signal attenuates with distance on a large scale.

n and $L_0(d_0)$ can be found by performing a linear regression. When $L_0(d)$ is found, it is simply replace in Equation 3.30 to find $L(d)$

It is found as shown in Figure 3.8 for M = 10 reflections that $n = 1.56$, and $L_0(d_0) = 50.59$dB

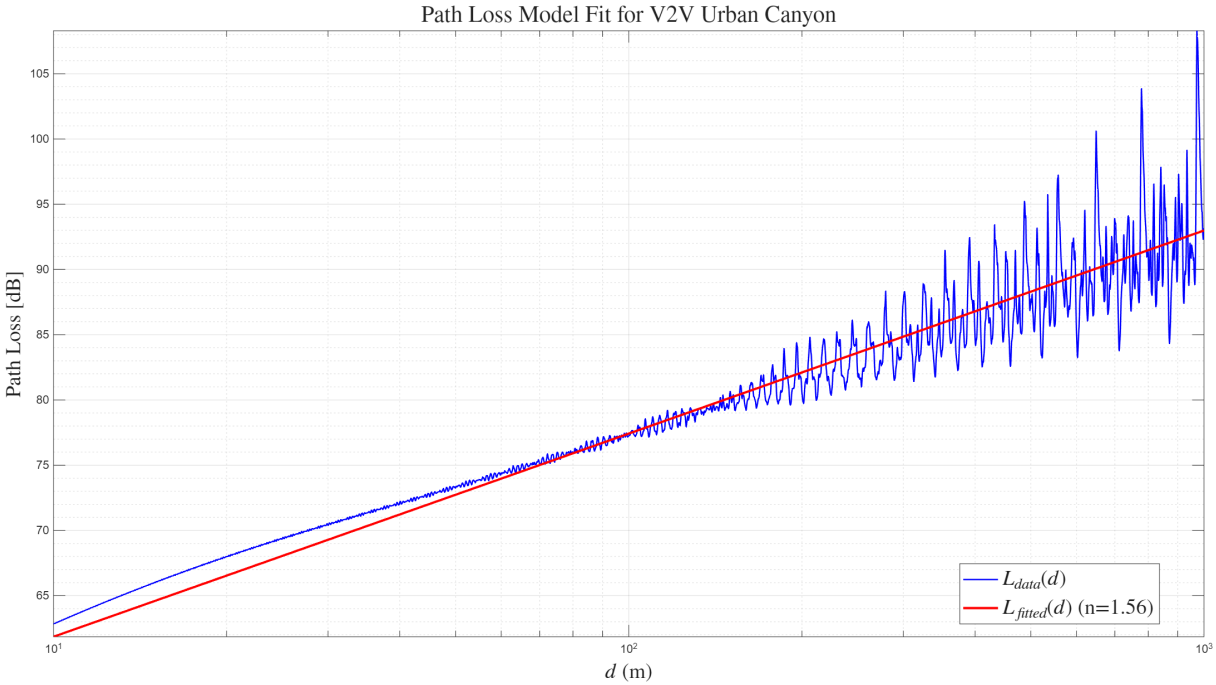

Figure 3.8: Path Loss Model Fitted, $M = 10$ reflections, $d_0 = 1$m

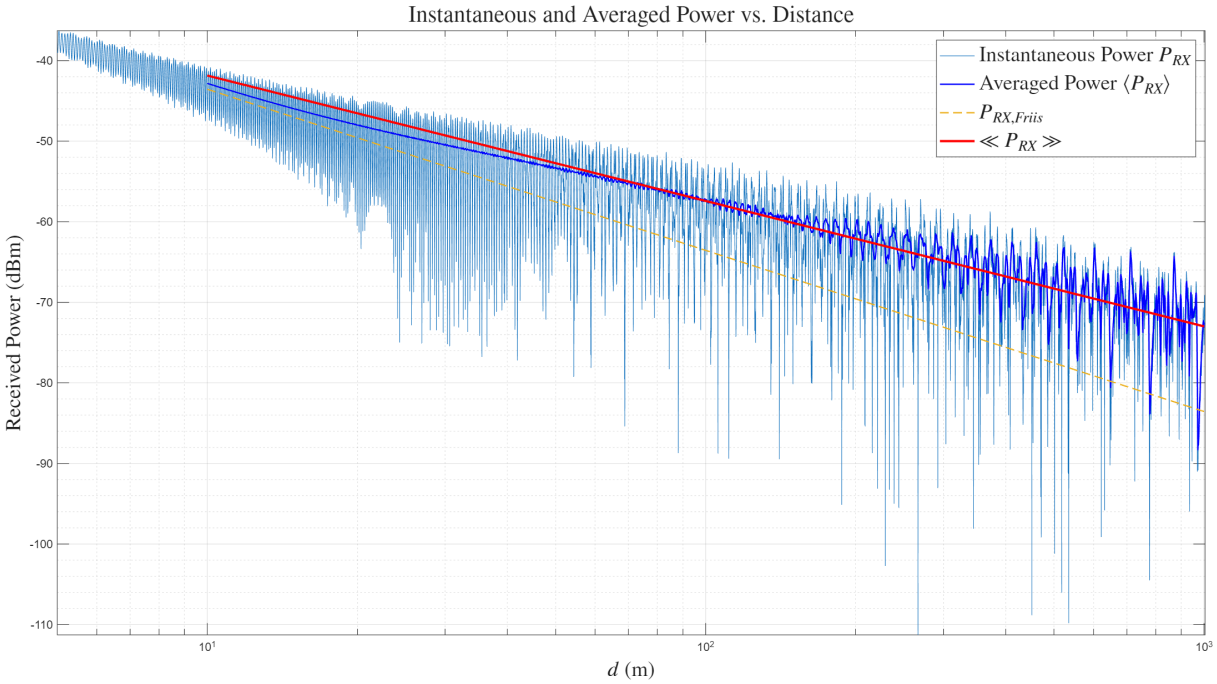

Figure 3.9: Power models, $M = 10$ reflections, $d_0 = 1$m

3.6 Variability σ_L

The shadowing standard deviation σ_L, quantifies the variation of the actual received power around the path loss model prediction. It is calculated as the standard deviation of the difference in dB between the local-area averaged power and the path loss model prediction.

$$\sigma_L^2 = \text{std}\left[\underbrace{L_{\text{data}}[\text{dB}] - L_{\text{fitted}}[\text{dB}]}_{\text{shadowing error}}\right] \tag{3.35}$$

$$\Longrightarrow \boxed{\sigma_L = 3.01\text{dB}} \quad (\text{for } M = 10 \text{ reflections}) \tag{3.36}$$

for $M = 10$reflections :

3.7 Fade Margin and Cell Range

The path loss model provides the large-scale averaged received power, $\ll P_{RX} \gg$. However, the local-area average power, $< P_{RX} >$, still fluctuates around this value due to shadowing. This phenomenon is modeled by considering $< P_{RX} >$ in dBm as a random variable following a normal distribution around $\ll P_{RX} \gg$ in dBm. The shadowing loss, L_{σ_L}, is therefore a zero-mean Gaussian random variable with a standard deviation of σ_L dB. To ensure reliable communication, a margin must be designed to counteract these random power drops.

The reliability of the system is the probability that the local-area average received power, $< P_{RX} >$, exceeds the receiver's sensitivity, which is the minimum required power threshold,

$P_{RX_{sens}} = -70\text{dBm}$.

$$\text{Reliability} = \Pr(< P_{RX} > \text{ greater than } P_{RX_{sens}}) \tag{3.37}$$

This condition can be expressed in terms of path loss. The total path loss experienced is the sum of the deterministic path loss from the model, $L(d)$, and the random shadowing loss, L_{σ_L}. For a successful connection, this sum must be less than the maximum allowed path loss, L_{max}, determined by the transmitter power and receiver sensitivity.

$$L(d) + L_{\sigma_L} < L_{max} \quad \text{where} \quad L_{max} = P_{TX}[\text{dBm}] - P_{RX_{sens}}[\text{dBm}] \tag{3.38}$$

To guarantee a specific reliability at the cell edge (range R), a **fade margin**, M, is introduced. This margin dictates that the deterministic path loss at the cell edge must be less than the maximum allowed path loss.

$$L(R) = L_{max} - M \tag{3.39}$$

Substituting this into the reliability condition reveals that for a successful connection at the cell edge, the random shadowing loss must be smaller than the fade margin.

$$(L_{max} - M) + L_{\sigma_L} < L_{max} \implies L_{\sigma_L} < M \tag{3.40}$$

The probability of an outage is the probability that the shadowing loss exceeds this margin. For a zero-mean Gaussian variable, this is given by the complementary error function (erfc), as shown in your course notes:

$$\text{Outage Probability} = \Pr(L_{\sigma_L} > M) = \frac{1}{2}\text{erfc}\left(\frac{M}{\sigma_L\sqrt{2}}\right) \tag{3.41}$$

The reliability is $1 -$ Outage Probability. The required fade margin M for a target reliability is found by inverting this expression:

$$M = \sigma_L\sqrt{2} \cdot \text{erfc}^{-1}(2(1 - \text{Reliability})) \tag{3.42}$$

Once M is determined, the maximum allowable antenna-independent path loss, $L_{0,max}$, can be calculated by removing the antenna gains from the total maximum path loss:

$$L_{0,max} = (P_{TX}[\text{dBm}] - P_{RX_{sens}}[\text{dBm}] - M) + 10\log_{10} G_{TX} + 10\log_{10} G_{RX} \tag{3.43}$$

$$= (20 \text{ dBm} - (-70 \text{ dBm}) - M) + 2.15 \text{ dBi} + 2.15 \text{ dBi} \tag{3.44}$$

$$= (90 - M) \text{ dB} + 4.3 \text{ dB} \tag{3.45}$$

$$\tag{3.46}$$

$$\implies \boxed{L_{0,max} = 94.3 - M} \quad [\text{dB}] \tag{3.47}$$

Finally, the cell range R is found by setting the fitted canonical path loss model from Equation (3.34) equal to this maximum value:

$$L_{0,max} = L_0(d_0) + 10n \log_{10}\left(\frac{R}{d_0}\right) \tag{3.48}$$

Solving for the cell range R gives:

$$R = d_0 \cdot 10^{\frac{L_{0,max} - L_0(d_0)}{10n}} \tag{3.49}$$

Using the path loss exponent $n = 1.56$, the shadowing standard deviation $\sigma_L =$ `[calculated_sigma_L]`, and the other system parameters, the fade margins and corresponding cell ranges are calculated for target reliabilities of 50%, 95%, and 99%.

Table 3.2: Fade margin and cell range for target reliabilities (M=10 reflections).

Reliability	**Fade Margin M [dB]**	**Cell Range R [m]**
50%	0.00	`[R_50]`
95%	`[M_95]`	`[R_95]`
99%	`[M_99]`	`[R_99]`

3.8 Interpretation of Results

The introduction of reflections from buildings fundamentally changes the channel behavior compared to the simple LOS case.

- **Multiray Fading:** The total received power is no longer a monotonic function of distance. The vector sum of the MPCs creates an interference pattern, causing rapid and deep fluctuations in signal strength (fading) as the distance d changes. This is a critical feature of real-world urban channels.
- **Rician K-factor:** The K-factor provides a quantitative measure of the channel's nature. For short distances d, the LOS ray is much stronger than the reflected rays, resulting in a high K-factor and a Rician-like distribution with moderate fading. As d increases, the LOS power decreases, and the reflected rays become relatively more significant, lowering the K-factor and making the channel behave more like a Rayleigh fading channel.
- **path loss Exponent:** The path loss exponent n derived from the averaged power will likely be greater than 2 (the free-space value). This is because the multiray environment

tends to confine the energy, creating a "waveguide" effect that can alter the rate of power decay with distance.

- **Fade Margin and Reliability:** The variability σ_L necessitates a fade margin to ensure reliable communication. A higher desired reliability (e.g., 99% vs. 95%) requires a larger fade margin, which in turn reduces the maximum communication range for the system. This highlights the trade-off between reliability and coverage in a fading channel.

3.9 LOS Channel - Wideband analysis

For the LOS channel, the impulsive h(τ) and H(f) are the same as written in **??** and **??** resp